Anisotropic bond percolation by position-space renormalisation group

1981 J. Phys. A: Math. Gen. 14 855

(http://iopscience.iop.org/0305-4470/14/4/015)

J. Phys. A: Math. Gen. **14** (1981) 855–871. Printed in Great Britain

Anisotropic bond percolation by position-space renormalisation group

Hisao Nakanishi†, Peter J Reynolds and Sidney Redner

Center for Polymer Studies‡ and Department of Physics, Boston University, Boston, MA 02215 USA

Received 13 August 1980

Abstract. We treat a percolation model with anisotropic bond occupation probabilities in order to study the crossover behaviour of the effective spatial dimension of the system. Previous position-space renormalisation group (PSRG) studies of this problem on the square lattice show a crossover from two-dimensional to pseudo-one-dimensional critical behaviour. To investigate the possible reasons for this surprising result, which is the opposite of the behaviour observed in thermal critical phenomena, we first develop alternative PSRG schemes. We study the predictions of these groups for asymptotically large rescaling parameters, where the approximations in the PSRG are thought to become negligible. From a consideration of the approximations involved, we are led to a decimation transformation that uses an anisotropic cluster. The results of this method indicate that anisotropic percolation is in the same universality class as isotropic percolation, in complete analogy with thermal critical phenoma. Our results indicate several peculiar features both of this problem and of the PSRG methods.

1. Introduction

The percolation problem has been pursued in recent years both for its direct relevance to various physical phenomena (e.g. the gelation transition — see de Gennes (1979), Coniglio *et al* (1979) and references therein), and for its correspondence with thermal critical phenomena (Kasteleyn and Fortuin 1969). In the thermal context, the idea of *crossover* has played an important role in our understanding of phase transitions (see e.g. Riedel and Wegner (1969), Aharony (1976) and references therein). Thus it is natural also to consider crossover behaviour in percolation. In particular, we study crossover between different spatial dimensionalities d, by treating *anisotropic* bond percolation§.

This model was first studied in $d = 2$ by Sykes and Essam (1963) who obtained the exact critical line. Temperley and Lieb (1971) later obtained the average number of clusters exactly along this critical line. More recently, Redner and Stanley (1979) have performed low-density series calculations for $d = 2$ and 3, and several exact calculations for all d. In addition, Ikeda (1979), Chaves *et al* (1979) and de Magalhães *et al* (1980)

† Present address: Baker Laboratory, Cornell University, Ithaca, NY 14853 USA.

‡ Supported in part by grants from ARO and AFOSR.

§ De Gennes (1979) has suggested that an unusual anisotropic gel may be produced by cross-linking hydrophilic polymer chains in the water layer of the lamellar phase of lipid + water.

0305-4470/81/040855+17$01.50

have studied this model on the square lattice by position-space renormalisation group (PSRG).

The results of PSRG studies appear surprising. Ikeda (1979) constrained the anistropy to be fixed under rescaling, and thus obtained a one-parameter group. For large anisotropy, he found the exponent ν to be much smaller than the isotropic value of about 1.3. Both Chaves *et al* (1979) and de Magalhães *et al* (1980) used the method of Reynolds *et al* (1977, 1980) with rescaling parameters $L = 2, 3$, and 4 and found that the isotropic fixed point is *completely* unstable. (Nevertheless, Chaves *et al* seem to give their results the interpretation that the isotropic fixed point still controls the critical behaviour of the anisotropic system.)

The series results also seem surprising. Redner and Stanley (1979) obtained the exact result $\phi_{1\to d} = 1$, for the exponent describing crossover from one- to d- (>1) dimensional behaviour. However, $\phi_{2\to 3}$, describing crossover from $d = 2$ to $d = 3$, was estimated by series to be about 1.75. This latter result is different from the value $\gamma_{d=2} \cong 2.4$ expected in analogy with anisotropic thermal critical phenomena. Here γ_d is the percolation analogue of the d-dimensional susceptibility exponent. Moreover, recently it was shown exactly that for anisotropic percolation in any dimension $\phi_{d-1\to d} = \gamma_{d-1}$ (Redner and Coniglio 1980). Thus, we have a case of a carefully analysed low-density series pointing to an incorrect result. It appears that perhaps the anisotropic percolation problem itself may have features difficult to analyse by conventional methods.

In order to put this in perspective, we recall that for the nearest-neighbour Ising ferromagnet on the square lattice, for arbitrary (finite) anisotropy, all the exponents are identical with the isotropic case. This follows from the exact calculation of the partition function (Onsager 1944), and from exact expressions for the two-spin correlation function for spins separated horizontally, vertically and diagonally (McCoy and Wu 1973). In the language of renormalisation groups, the isotropic Ising fixed point is stable with respect to anisotropy. Moreover, scaling analysis (Abe 1970, Suzuki 1971) and momentum-space RG (Aharony 1976) agree with the exact results in the case of the two-dimensional Ising model, and yield analogous results in higher dimensions. We believe these arguments can be carried over to the present case of bond percolation by using the Potts mapping (Kasteleyen and Fortuin 1969).

Therefore, we have a situation in which neither series expansions nor PSRG gives a satisfactory result. In particular, the latter seems to yield an incorrect *direction* for the crossover. To address this point we present several PSRG treatments. Careful analysis indicates that the isotropic fixed point is in fact stable, and that the direction of the crossover is the same as in the thermal case. First we examine the cell PSRG method of Reynolds *et al* (1977), and show that this procedure is inadequate for describing anisotropic percolation. We therefore formulate alternative PSRG methods, and indicate how it is possible systematically to improve upon these approximations. Finally, we present a decimation procedure based on an anisotropic cluster, which predicts RG flows consistent with the thermal case. Our recursion relations are presented in appendix 1.

2. Position-space renormalisation group in two dimensions

In the following, we treat anisotropic bond percolation on the square lattice, with horizontal and vertical bonds occupied with probabilities a and b, respectively.

2.1. *Cell* PSRG

In the cell PSRG scheme of Reynolds *et al* (1977), one considers an $L \times L$ cell (cf figure 1(a)), and obtains renormalised probabilities a' and b' by the criteria that configurations with horizontally or vertically spanning paths contribute to a' and b' respectively.

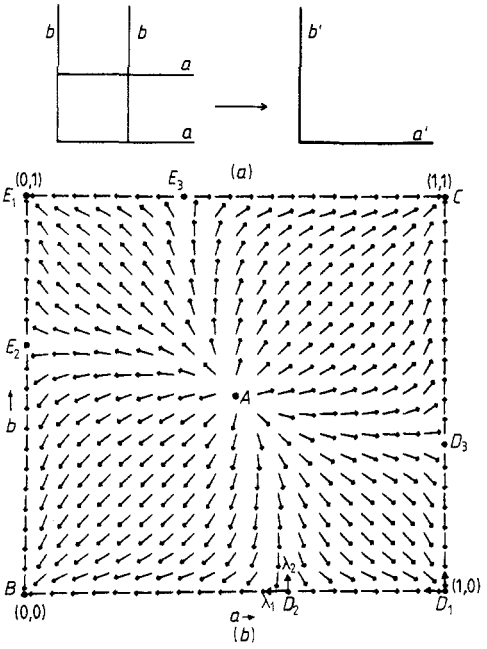

Figure 1. (a) The 2×2 bond cell. This cell rescales to a single horizontal and vertical bond (shown to the right) upon renormalisation. (b) Renormalisation group flows based on the recursion relation for the cell in (a). At the fixed points D_1 and D_2, the eigenvectors are sketched. The eigenvalues are defined according to the notation used in the paper.

For example, in the case of $L = 2$ we have

$$a' = a^4 + 4a^3(1-a) + 4a^2(1-a)^2 b + 2a^2(1-a)^2(1-b) \equiv f(a, b),$$
$$b' = f(b, a). \tag{1}$$

This leads to the flow diagram shown in figure 1(b). Some unexpected features of this diagram are: (1) the isotropic fixed point A at $(a, b) = (\frac{1}{2}, \frac{1}{2})$ is unstable in all directions, and (2) the two one-dimensional fixed points, that should appear at (1, 0) and (0, 1), are each split into three fixed points, D_1, D_2, D_3 and E_1, E_2, E_3 respectively.† Notice further that by symmetry ($a \leftrightarrow b$) and by duality ($a \leftrightarrow 1-b$) the phase diagram of figure 1(b) is symmetric about the two diagonals of the square.

Let us consider first the properties near the isotropic fixed point A. For rescaling parameters $L = 2$, 3 we have calculated the matrix of derivatives

$$T_L^{\alpha'\beta}(A) = (\partial\alpha'/\partial\beta)_L|_A \tag{2}$$

† These features remain unchanged even if the cell is placed on a cylinder or a torus to impose periodic boundary conditions.

in order to calculate the recursion relations linearised about A. Here α, β denote a or b. For $L = 2$ we obtain

$$T_2(A) = \begin{bmatrix} \frac{3}{2} & \frac{1}{8} \\ \frac{1}{8} & \frac{3}{2} \end{bmatrix},$$

whose normalised eigenvectors are $\psi_1 = (1/\sqrt{2})[^1_1]$ and $\psi_2 = (1/\sqrt{2})[^1_{-1}]$; the eigenvalues are $\lambda_1(A) = \frac{13}{8}$ and $\lambda_2(A) = \frac{11}{8}$ respectively. Thus, the corresponding scaling powers $y_i(A) = \ln \lambda_i / \ln L$ are both positive, with values of 0.70 and 0.46 respectively. One might expect that the latter scaling power becomes negative as $L \to \infty$, so that the isotropic fixed point will ultimately become stable with respect to anisotropy (the ψ_2 direction). However, this scaling power appears to remain positive for any finite L. In particular, for $L = 3$, the scaling powers associated with the eigenvectors ψ_1 and ψ_2 are 0.73 and 0.38, and a naive extrapolation against $1/\ln L$ yields $y_2(A) = 0.24$ in the limit $L \to \infty$.

Consider now the remaining non-trivial fixed points. The spurious fixed points arise from the nature of the system at $(a, b) = (1, 0)$ and $(0, 1)$. These limits are not simple one-dimensional systems, but rather have the percolation characteristics of L independent parallel chains. Chaves *et al* (1979) and de Magalhães *et al* (1980) noted that the 'spurious' fixed points, D_2, D_3 and E_2, E_3, converge to $(1, 0)$ and $(0, 1)$ respectively as $L \to \infty$. However, no significance was attached to the unusual critical behaviour predicted by the flow diagram for any finite L. Moreover, we find that the scaling powers in the $L \to \infty$ limit appear to depend on how rapidly the spurious fixed points approach $(1, 0)$ and $(0, 1)$. To understand this situation, we study in detail the RG properties for large L near the six 'one-dimensional' fixed points. We are able to do this because the full recursion relations (cf equation (1)) simplify greatly near these fixed points. For example, consider the equation for a': if we arrange the terms in ascending order in the number of a bonds, we have

$$a' = a^L(1-a)^{L^2-L}P_L(b) + \cdots + a^{L^2-L}(1-a)^L P_{L^2-L}(b) + Q(a), \tag{3}$$

where the $P_i(b)$ are polynomials in b. Here $Q(a)$ contains the contribution to the recursion relation due to all configurations with more than $(L^2 - L)$ a bonds. (Thus no b bonds are required for connectivity across the configurations included in $Q(a)$, see for example equation (1).) Since $Q(a) = a^{L^2} + L^2 a^{L^2-1}(1-a) + \ldots$, we find

$$(\partial a'/\partial a)|_{a=1} = (\partial a'/\partial b)|_{a=1} = 0 \tag{4a}$$

and

$$(\partial a'/\partial a)|_{a=0} = (\partial a'/\partial b)_{a=0} = 0 \tag{4b}$$

as well as

$$a'|_{a=1} = 1, \qquad a'|_{a=0} = 0. \tag{5}$$

By the symmetry of $a' = f(a, b)$, $b' = f(b, a)$, the derivatives of b' with respect to a and b evaluated at $b = 1$ and $b = 0$ are also equal to zero. This symmetry also gives $b'|_{b=1} = 1$ and $b'|_{b=0} = 0$. Thus the flow along any edge of the square is confined to that edge (figure 1). Moreover,

$$T_L(B) = T_L(C) = T_L(D_1) = T_L(E_1) = \mathbf{0} \tag{6}$$

for all L. In other words B, C, D_1 and E_1 are infinite 'sinks' for all cell sizes.

Similar simplifications apply for points D_2, D_3 and E_2, E_3. Consider, for example, D_2. Here $b^* = 0$ and a^* is given by the non-trivial solution of the recursion relation for L independent chains to percolate,

$$a' = 1 - (1 - a^L)^L. \tag{7}$$

The existence of the spurious fixed point predicted by equation (7) may be understood by the following argument which illustrates the approximation in the cell PSRG. Two adjacent 2×2 cells, each with two occupied a bonds (cf figure 2) renormalise into two neighbouring occupied bonds. After a second rescaling, these renormalise into a single occupied bond. However, the original bond configuration does not form a spanning configuration across the two cells. Thus our approximation overcounts intercell connections by including paths which are actually on different chains, overestimating a', hence giving rise to a fixed point D_2 at a value $a^* < 1$. Notice also that, due to the presence of D_2, D_1 is stable with respect to perturbations in a. By duality ($a \leftrightarrow 1 - b$), this situation occurs in the vertical direction also. Thus D_1 is stable in all directions, and this holds for all L.

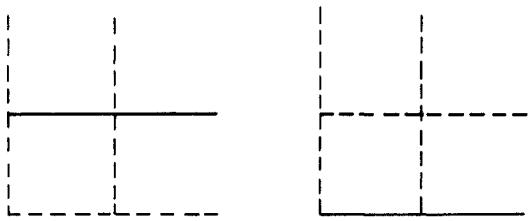

Figure 2. Two adjacent 2×2 cells in which the bonds span across each cell, but not across both cells.

From equation (7), it is easy to see that a^* approaches unity (i.e. $D_2 \to D_1$) as the cell size increases. However, we are interested in how rapidly this occurs, and also in the behaviour of the flow diagram as $L \to \infty$. An analysis of this is presented in appendix 2. We find that although the spurious fixed points converge toward the correct one-dimensional limits, the scaling powers do not approach the expected values. The isotropic fixed point remains unstable for all L. Since the large-cell limit of this scheme can be interpreted as computing the connectivity properties exactly for a large but finite system, the 'backward' flows seem to indicate a peculiar feature of the anisotropic problem. It appears that a cell approach, which inherently has parallel one-dimensional chains as its extreme anisotropic limits, is not sufficiently sensitive on a global scale to give correct asymptotic behaviour. Before we discuss this difficulty in more detail, we first develop some alternative PSRG schemes.

2.2. Decimation

Turban (1979) noted that the usual decimation method which renormalises the square cluster of figure 3(a) into the two-site cluster in figure 3(b) is not appropriate for anisotropic percolation. This is because a renormalised bond cannot be interpreted as being either horizontal or vertical, and as a result the renormalised problem becomes isotropic. To overcome this difficulty, we propose a decimation scheme which takes the cluster of figure 3(c), and renormalises it to the cluster of figure 3(d), so that the

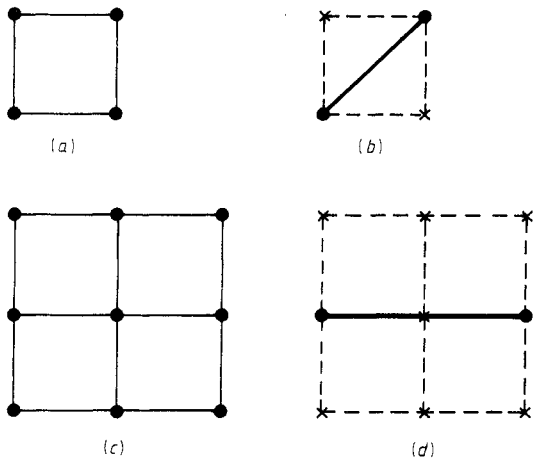

Figure 3. The four-site cluster (*a*) which rescales to the two-site cluster (*b*) upon decimation. This is appropriate only for isotropic bond percolation. We show in (*c*) the nine-site, $L = 2$ cluster, and its renormalised counterpart in (*d*), that we use for a decimation treatment of anisotropic bond percolation.

directionality of the bonds is preserved. This method avoids the problem of having connectivity of many chains in the extreme anisotropic limit, and mitigates some of the intercell connectivity problems discussed previously. It also allows for longer paths to contribute to connectivity than in the cell approach for the same rescaling parameter L. The resulting recursion relations for $L = 2$ are given in appendix 1, and the flow diagram is shown in figure 4.

The global features of this diagram are somewhat different from those given by the cell PSRG. The isotropic fixed point A is now *stable* with respect to anisotropy, and only two pseudo-one-dimensional fixed points appear. The stability is now consistent with lattice-dimensionality crossover from the anisotropic system to the isotropic higher-dimensional system. The splitting of the one-dimensional fixed points, however, is still

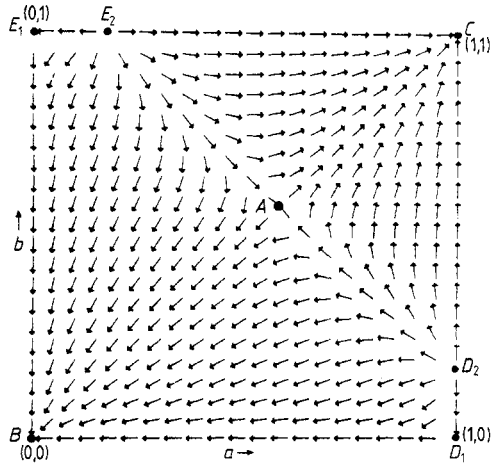

Figure 4. Renormalisation group flows based on the recursion relation for decimation of the nine-site cluster of figure 3(*c*).

similar to what occurs in the cell PSRG. Furthermore, although the recursion relations for our decimation procedure (given in appendix 1) are symmetric under the exchange $(a \leftrightarrow b)$, duality arguments do not apply here. Thus, the symmetry $(a \leftrightarrow 1-b)$ is lacking.

We can obtain more information on the edges of the square, where we can study the properties of the linearised recursion relations at D_2 asymptotically for large L (cf appendix 3). We find that the scaling power y_1 (corresponding to the larger eigenvalue) approaches the one-dimensional value of unity, and its right eigenvector† approaches $\begin{bmatrix}-1\\0\end{bmatrix}$. The scaling power y_2 goes to zero, making the eigenvector $\begin{bmatrix}0\\1\end{bmatrix}$ marginal in the asymptotic limit. Thus, if we were to compute an approximation to the crossover exponent by taking $\lim_{L\to\infty} y_2/y_1$, we would obtain zero. Therefore the decimation method also has difficulties in converging quantitatively to the correct $L \to \infty$ limit. However, the qualitative behaviour of the one-dimensional limit and the direction of the crossover are one consistent with our expectations from thermal critical phenomena.

2.3. PSRG on the q-state Potts model with $q \to 1$

Because of these failures in the direct PSRG methods, it is of interest to consider a very different approach. For this reason we apply the PSRG of Niemeijer and van Leeuwen (1976) to the q-state Potts model, and then take the percolation limit of $q \to 1$ (Kasteleyn and Fortuin 1969). Clearly, it is a disadvantage that our intuition—based on direct configurational ideas of connectivity—is not applicable here. However, this disadvantage may be offset by using a formalism in which there is a partition function that may be left invariant under the RG. It is of interest also to see whether the apparent difficulties associated with anisotropic percolation are confined to the direct PRSG methods, or whether the difficulties reflect particular properties of the problem itself.

Our results, however, are difficult to interpret. The first-order cumulant approximation, with a weight function based on a proportionality rule plus connectivity on a 2×2 cell‡, results in a line of fixed points in place of a crossover line (cf figure 5(a)). Hence the behaviour is now *not* universal, with the exponents varying along the critical line. In spite of this behaviour, the cumulant expansion gives the reasonable results of $p_c = 0.52$ and $\nu = 1.9$ in the isotropic limit. A two-cell cluster RG with the same weight function, however, leads to a stable isotropic fixed point and *no* fixed line. Unfortunately, no fixed points appear that correspond to any one-dimensional limits (cf figure 5(b)). We do not fully understand why this is so: it may simply be due to the lowest-order approximation we used, or to the particular weight function. In this connection, we find that the first-order cumulant approach does not work well for the anisotropic $q = 2$ (Ising) case either. Thus it may well be that cell PSRGs fail to describe aniostropic systems adequately.

2.4. Discussion of § 2.1–2.3

The various PSRG methods we have treated thus far all appear to fail. In the case of the

† We consider the right eigenvectors here instead of the usual left eigenvectors, since we are interested in those vectors that lie tangent to the critical surface.

‡ Our rule reduces to the proportionality rule if there is no spanning path of one species; if there is one spanning species, then the cell is assigned that species, while if there are two spanning species, the cell has probability $\frac{1}{2}$ of having one or the other of those species.

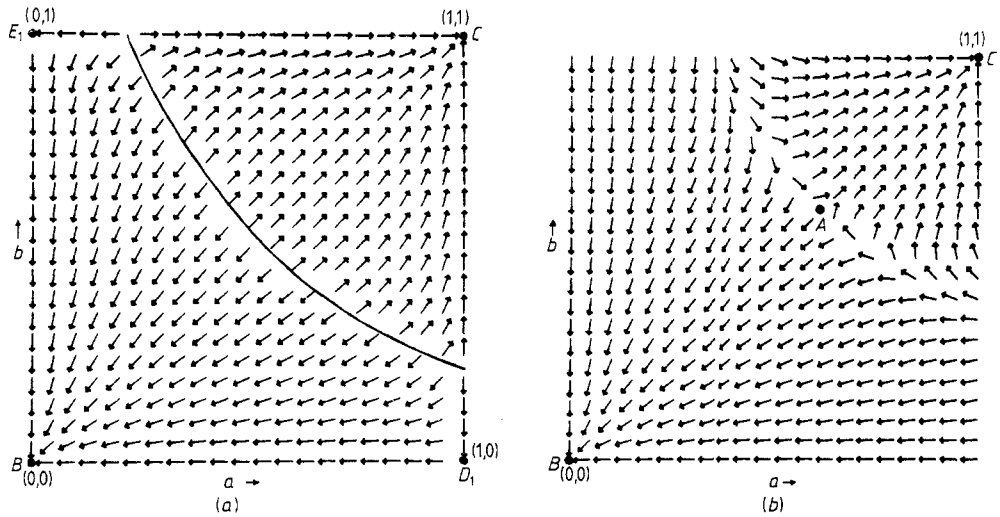

Figure 5. (*a*) Renormalisation group flows obtained from the recursion relation using the first-order cumulant approximation with 2×2 cells in the q-state Potts model after the limit $q \to 1$ has been taken. (*b*) Renormalisation group flows based on a two-cell cluster treatment of the q-state Potts model.

cell PSRG, we have argued that the incorrect one-dimensional limits of multiple parallel paths are the essential cause of the spurious fixed points. Since this is a problem of overestimating connectivity over the distance scale of several cells, it persists even if the boundaries are artificially removed by imposition of periodic boundary conditions. In addition, although these spurious fixed points do converge to the 'correct' locations as $L \to \infty$, the convergence is so slow that the eigenvalues fail to approach the correct asymptotic limits (cf appendix 2). On the other hand, any finite cell approximation also underestimates connectivity, because it does not contain the long, contorted paths that are important for global connectivity. The overestimation previously mentioned and this underestimation are generally not related since they are caused by totally different effects†; nor are they likely to cancel.

The decimation approach discussed in § 2.2 is an attempt to overcome the intercell difficulties, since decimation uses no cells, but rather sums over the degrees of freedom associated with certain sites within a cluster. The resulting method has the correct direction of the dimensional crossover, as well as the correct one-dimensional limits. However, two spurious fixed points persist, which arise from underestimation of connectivity due to the large, contorted paths which are not included. For example, on the axis $a = 1$, we always have a fixed point $b^* > 0$ for finite cell size. However, $a = 1$, $b > 0$ implies an infinite connectivity in both the a and b directions, however small b may be. Thus, the correct fixed point should be at $b^* = 0$. This shows that neglecting the paths that go beyond the cluster is a severe approximation for a decimation scheme in the case of anisotropic percolation. Although the spurious fixed points coalesce with the pseudo-one-dimensional fixed points as $L \to \infty$, and although the direction of the

† It is interesting to note, however, that for the cell PSRG of § 2.1, these two 'opposite' effects are in fact related by duality (although they still do not cancel). This is reflected in the fact that the fixed points D_2 and D_3 are symmetric about the line $a + b = 1$ in figure 1(*b*). However, for decimation there is no duality, and the symmetry between D_2 and D_3 is broken.

crossover is correct, the limiting behaviour of the scaling powers is still not the correct one-dimensional limit. This latter situation is similar to that encountered in the cell PSRG.

In contrast, an entirely different approach based on the Potts model mapping leads to its own difficulties. Here, the inapplicability of the direct configurational ideas does not permit us to make any general comments; however, it does seem possible that conventional cell approaches are inadequate to describe the anisotropic system.

2.5. Anisotropic decimation

In order to include some of the paths which were previously not included, we introduce an anisotropic cluster. In this case we find that — even for fixed L — taking the extreme anisotropic limit of the cluster provides sufficiently fast convergence that the limiting scaling powers are correct. For example, using a $2\times n$ cluster with n even, and a rescaling parameter of $L=2$ (cf figure 6 (a)), we find for the recursion relation on the $a=1$ axis

$$b^* = [1-(1-b^*)^{n+1}]^2 \tag{8}$$

or

$$b^* \sim 1/n^2.$$

At the fixed point D_2 (figure 6(b)), we have

$$T_{2,n}(D_2) = \begin{bmatrix} \lambda_1 & 0 \\ X & \lambda_2 \end{bmatrix}. \tag{9}$$

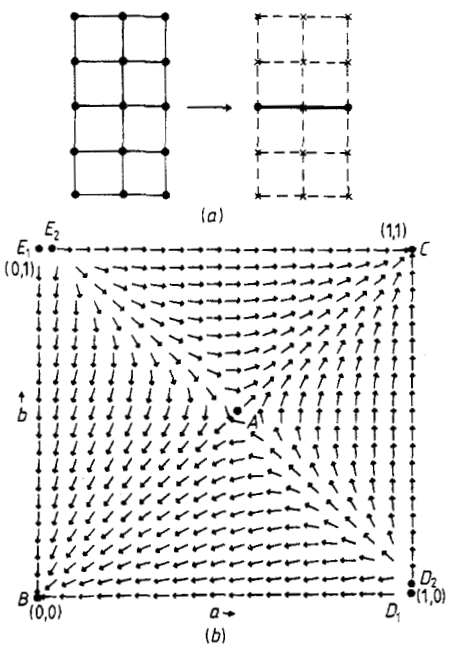

Figure 6. (a) 4×2, 15-site cluster used for anisotropic decimation. The resulting two-site cluster after rescaling is shown to the right. (b) The renormalisation group flows from the anisotropic decimation procedure.

Following arguments similar to those in appendix 3, it can be shown that

$$\lambda_1 \equiv (\partial a'/\partial a)\big|_{\substack{a=1 \\ b=b^*}} = 2\{1-b^*[1-(1-b^*)^2]\}^2 \tag{10a}$$

and

$$\lambda_2 \equiv (\partial b'/\partial b)\big|_{\substack{a=1 \\ b=b^*}} = 2(n+1)(1-b^*)^n[1-(1-b^*)^{n+1}]. \tag{10b}$$

Since $b^* \sim 1/n^2$, these results yield $\lambda_1 \to 2$ and $\lambda_2 \to 2$ as $n \to \infty$, and thus the associated scaling powers obey $y_1 \to 1$ and $y_2 \to 1$. By calculations similar to those in appendix 3, we also obtain

$$X \to -2. \tag{11}$$

Both (right) eigenvectors collapse onto $\begin{bmatrix}0\\1\end{bmatrix}$ asymptotically (i.e. as $n \to \infty$). Since the other eigendirection is associated with the eigenvector $\begin{bmatrix}1\\0\end{bmatrix}$ at the fixed point D_1, with $\lambda_0 = 2$, we have

$$\phi = \lim_{n\to\infty} y_2/y_0 = 1. \tag{12}$$

Thus, this RG reproduces the correct crossover exponent $\phi_{1\to d}$, in addition to the features that were already correct in the isotropic decimation scheme. The recursion relations for $n = 4$ are given in appendix 1, and the resulting flow diagram is shown in figure 6(b).

3. Three and higher dimensions

Next, we consider systems of higher dimensionality. As an example, we treat the simple cubic lattice by the cell PSRG. Bonds in the x, y, and z directions are occupied with probabilities a, b, and c respectively. Figure 7(a) shows the $2\times2\times2$ cell used, and the resulting recursion relations are given in appendix 1. We show a section of the flow diagram for $b = c$ (thus $b' = c'$) in figure 7(b).

The similarities of this figure to figure 1(b) for the square lattice are striking. The fixed point A now has the three-dimensional isotropic symmetry $a = b = c$, while E is the isotropic pseudo-two-dimensional fixed point. The fixed points D_2 and D_3 represent the pseudo-one-dimensional fixed points that split off from the fixed point D_1. A similar situation occurs for the fixed points F_1 and F_2. According to the flow diagram, crossover between $d = 1$ and $d = 3$, as well as between $d = 2$ and $d = 3$, is in the direction of decreasing dimensionality, in the same manner as in the cell PRSG approach in two dimensions.

In higher dimensions, the results look very similar. We use Monte Carlo techniques to obtain renormalised probabilities from a set of unrenormalised ones. In particular, to consider the crossover between d and $(d-1)$ dimensions, we need only study the cross section $p_1 = p_2 = \ldots = p_{d-1} \equiv p$ (where subscripts refer to directions). This cross section can be represented by a unit square (p, p_d), and the $(d-1)$-dimensional fixed point appears on the p axis while the isotropic d-dimensional fixed point appears on the line $p = p_d$. We should thus study the stability of the $(d-1)$-dimensional fixed point by looking at the directions of flows near it along the p axis (particularly the p_d projection). For example, in six dimensions with a 2^6-site cell, we find that out of 13,000 realisations

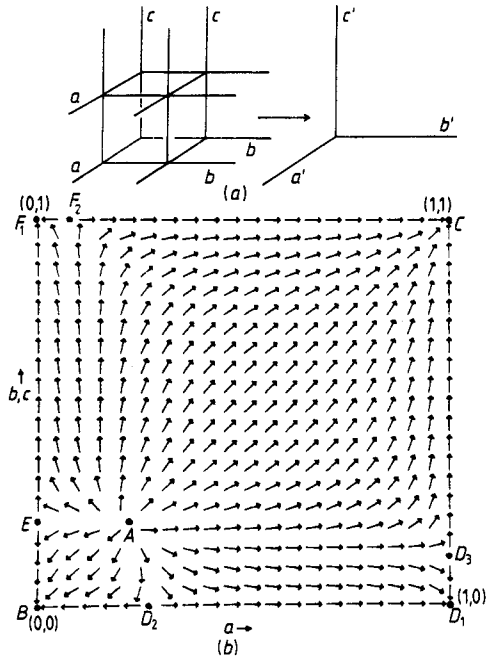

Figure 7. (*a*) The $2 \times 2 \times 2$ cell used to study bond percolation on the simple cubic lattice. On the right we show the resulting cell after one rescaling. (*b*) The normalisation group flows based on the cell in (*a*).

generated at $p_1 = p_2 = p_3 = p_4 = p_5 = 0.12$, $p_6 = 0.01$, only 101 percolate in the p_6 direction, giving $p_6' = 0.008 < p_6$. Thus it appears that the six-dimensional isotropic fixed point is unstable, and crossover to pseudo-five-dimensional behaviour occurs. This method can be applied to arbitrary dimensions, and the global flows may be obtained in this way.

These results may be understood in the same way as our above results in two dimensions: we overestimate p' due to the many parallel hyperplanes (thereby overestimating the intercell connections). Nevertheless we also underestimate p' due to the omission of long-range, contorted paths. In addition to these approximations, the nature of the infinite cluster(s) in high dimensions may be quite different from that in $d = 2$ or 3, even for the isotropic problem. For example, it is not known rigorously whether there is only one infinite cluster for large d (Newman and Schulman 1979, unpublished). This potential new feature may have important ramifications on the application of a PSRG approach. Thus more studies in this area will be required to understand the effect of anisotropy for large dimensionalities.

4. Summary

We have treated bond percolation with anisotropies in the bond occupation probabilities to study the crossover behaviour of the effective system dimensionality. Various PSRG approaches for the square lattice were developed, and attempts were made to explain the apparent crossover to lower dimensionality predicted by the cell PSRG approach. We present evidence that these results are not inconsistent with

anisotropic percolation for finite anisotropy belonging to the same universality class as the isotropic problem. This is because the incipient infinite connectivities in both horizontal and vertical directions — at a point on the critical line $a+b=1$ — are quite sensitive to the approximations used in the cell PSRG approaches. Thus the approximations need to be dealt with in a systematic way to see ultimately the universal behaviour. To this end, we proposed a decimation method on an anisotropic cluster. This procedure yields results fully consistent with thermal critical phenomena.

Acknowledgments

It is a pleasure to thank Antonio Coniglio, Bill Klein, Gene Stanley and Julia Yeomans for interesting discussions. We are particularly grateful to Gerald Shlifer and Constantino Tsallis for communicating their related work to us and for stimulating conversations.

Appendix 1. Recursion relations

For decimation using a 2×2 cluster, we find the recursion relations

$$\begin{aligned} a' &= a^6 + a^5(1-a)(6A_6+36A_5+88A_4+107A_3+68A_2+24A_1+4A_0) \\ &\quad + a^4(1-a)^2(15A_6+86A_5+190A_4+199A_3+112A_2+36A_1+6A_0) \\ &\quad + a^3(1-a)^3(18A_6+92A_5+170A_4+156A_3+80A_2+24A_1+4A_0) \\ &\quad + a^2(1-a)^4(9A_6+34A_5+53A_4+44A_3+21A_2+6A_1+A_0) \\ &\equiv f_1(a,b), \qquad\qquad (A1.1) \\ b' &= f_1(b,a), \end{aligned}$$

where A_i denotes $b^i(1-b)^{6-i}$.

In the case of *anisotropic* decimation, the complete recursion relation for $n=4$, $L=2$ is

$$\begin{aligned} a' &= a^{10} + a^9(1-a)(10B_{12}+120B_{11}+658B_{10}+2175B_9+4820B_8+7541B_7+8546B_6 \\ &\quad + 7081B_5+4270B_4+1835B_3+536B_2+96B_1+8B_0) \\ &\quad + a^8(1-a)^2(45B_{12}+540B_{11}+2948B_{10}+9621B_9+20\,846B_8+31\,613B_7 \\ &\quad\qquad +34\,536B_6 \\ &\quad + 27\,541B_5+16\,016B_4+6670B_3+1902B_2+336B_1+28B_0) \\ &\quad + a^7(1-a)^3(120B_{12}+1436B_{11}+7763B_{10}+24804B_9+52\,027B_8+75\,828B_7 \\ &\quad + 79\,436B_6+60\,847B_5+34\,140B_4+13\,806B_3+3852B_2+672B_1+56B_0) \\ &\quad + a^6(1-a)^4(210B_{12}+2488B_{11}+13\,161B_{10}+40\,601B_9+81\,492B_8+11\,3354B_7 \\ &\quad + 113\,519B_6+83\,483B_5+45\,250B_4+17\,804B_3+4870B_2+840B_1+70B_0) \\ &\quad + a^5(1-a)^5(250B_{12}+2892B_{11}+14683B_{10}+42959B_9+81591B_8+107758B_7 \\ &\quad + 103018B_6+72800B_5+38192B_4+14651B_3+3936B_2+672B_1+56B_0) \end{aligned}$$

$$
\begin{aligned}
&+a^4(1-a)^6(200B_{12}+2204B_{11}+10445B_{10}+28434B_9+50667B_8+63375B_7\\
&\quad+57877B_6+39384B_5+20046B_4+7514B_3+1986B_2+336B_1+28B_0)\\
&+a^3(1-a)^7(100B_{12}+1000B_{11}+4256B_{10}+10\,632B_9+17\,718B_8+21\,012B_7\\
&\quad+18\,380B_6+12\,080B_5+5982B_4+2196B_3+572B_2+96B_1+8B_0)\\
&+a^2(1-a)^8(25B_{12}+200B_{11}+744B_{10}+1700B_9+2657B_8+3000B_7+2524B_6\\
&\quad+1608B_5+777B_4+280B_3+72B_2+12B_1+B_0)\\
&\equiv f_2(a,b), \qquad\qquad (A1.2)\\
&\qquad b'=f_2(b,a),
\end{aligned}
$$

where B_i denotes $b^i(1-b)^{12-i}$.

For the cell PSRG in three dimensions, using the $2\times2\times2$ cell we obtain the recursion relations

$$
\begin{aligned}
a'=a^8&+8a^7(1-a)+28a^6(1-a)^2+56a^5(1-a)^3\\
&+2a^4(1-a)^4(68C_{22}+136C_{21}+136C_{12}+66C_{20}+264C_{11}+66C_{02}\\
&+124C_{10}+124C_{01}+54C_{00})+8a^3(1-a)^5(48C_{22}+96C_{21}+96C_{12}\\
&+40C_{20}+168C_{11}+40C_{02}+64C_{10}+64_{01}+24C_{00})+4a^2(1-a)^6\\
&\times(16C_{22}+32C_{21}+32C_{12}+8C_{20}+40C_{11}+8C_{02}\\
&+12C_{10}+12C_{01}+4C_{00})\\
&\equiv f_3(a,b,c),\\
&\quad b'=f_3(b,c,a), \qquad\qquad (A1.3)\\
&\quad c'=f_3(c,a,b),
\end{aligned}
$$

where C_{ij} denotes $b^i(1-b)^{2-i}c^j(1-c)^{2-j}$.

Appendix 2. Large-L behaviour of the cell PSRG

To study the $L\to\infty$ behaviour of the pseudo-one-dimensional fixed points found in the cell PSRG approach, let us define $r=1-a^*$. Then equation (7) becomes

$$r=[1-(1-r)^L]^L. \qquad (A2.1)$$

By considering the graph of the right-hand side of (A2.1), it is easy to show that $r\to0$ as $L\to\infty$. However, we are interested in how fast this occurs. Thus, let us first suppose $r\to0$ faster than $1/L$ (or $Lr\to0$). If we then expand the quantity of brackets on the right-hand side of (A2.1), we have

$$
\begin{aligned}
1-(1-r)^L&=Lr+L(L-1)r^2/2+\cdots+(-1)^{L-1}r^L\\
&\equiv C_L Lr.
\end{aligned}
$$

Note that, because of our assumption that $Lr\to0$,

$$C_L\to1 \text{ as } L\to\infty.$$

From (A2.1), this would then imply

$$Lr^{1-1/L} \to 1$$

which is a contradiction to our assumption $Lr \to 0$. Thus we deduce that r goes to zero no faster than $1/L$. We write

$$r = (1/L)(1/\phi(L)), \tag{A2.2}$$

and consider the asymptotic behaviour of $\phi(L)$. Since r does not go to zero faster than $1/L$, $\phi(L)$ is bounded. Hence, assuming no pathological oscillations, $\phi(L)$ must converge to some number $\phi(\infty)$. Then, we have $r^{1/L} \to 1$ as well as $1-(1-r)^L \to 1-\exp[-1/\phi(\infty)]$. Equating these, we obtain $\phi(\infty) = 0$. We conclude therefore that $L\phi(L) \to \infty$, but $\phi(L) \to 0$ as $L \to \infty$. Furthermore, by rewriting (A2.1) and (A2.2) as

$$L\phi(L)[1-(1-r)^L]^L \sim \exp\{\ln L + \ln \phi(L) - L \exp[-1/\phi(L)]\} \to 1$$

and by noting that $\ln L + \ln \phi(L) = \ln L\phi(L)$ is still dominated by $\ln L$ (because $L\phi(L) \to \infty$), we can finally obtain

$$\phi(L) \sim 1/(\ln L - \ln \ln L). \tag{A2.3}$$

Thus the asymptotic behaviour of the fixed point is

$$a^* \sim 1 - (\ln L - \ln \ln L)/L. \tag{A2.4}$$

To obtain similar expressions for the asymptotic scaling powers, we consider D_2 and calculate the matrix

$$T_L(D_2) = \begin{bmatrix} \lambda_1 & X \\ 0 & 0 \end{bmatrix} \tag{A2.5}$$

where

$$\lambda_1 = (\partial a'/\partial a)|_{D_2} = L^2(1-a^*)/(1-a^{*L})a^{*L-1} \tag{A2.6}$$

and

$$X = (\partial a'/\partial b)|_{D_2}. \tag{A2.7}$$

At D_2 we find that the relevant eigenvalue λ_1 is associated with the (right) eigenvector $\begin{bmatrix} 1 \\ 0 \end{bmatrix}$, and the irrelevant eigenvalue λ_2 (=0) with the direction $\begin{bmatrix} -1 \\ \lambda_1/X \end{bmatrix}$ (cf figure 1(*b*)). For $L = 2$, $\lambda_1 = 1.53$, leading to a scaling power $y_1 = 0.612$. For $L = 3$, $\lambda_1 = 1.95$ and $y_1 = 0.608$. The asymptotic expression for y_1 is given by

$$y_1 \sim 1 - (\ln \phi(L)/\ln L) - 1/(\phi(L) \ln L) \sim 2 \ln \ln L/\ln L \to 0 \text{ as } L \to \infty. \tag{A2.8}$$

However, this scaling power is associated with the eigenvector along the $b = 0$ axis at the fixed point D_2, and this ought to approach the one-dimensional value of $1/\nu_{d=1} = 1$ as D_2 approaches (1, 0).

The eigenvector $\begin{bmatrix} -1 \\ \lambda_1/X \end{bmatrix}$ can also be computed for large L. We have

$$\begin{aligned} X &= (\partial/\partial b)[(1-b)^{L^2} G_0(a) + b(1-b)^{L^2-1} G_1(a)]_{a=a^*,\, b=0} \\ &= -L^2 G_0(a^*) + G_1(a^*), \end{aligned} \tag{A2.9}$$

where $G_0(a)$ and $G_1(a)$, the contributions to a' with zero and one vertical bond respectively, are

$$G_0(a) = 1 - (1-a^L)^L,$$

$$G_1(a) = [L^2 - (L-1)^2]G_0(a) + (L-1)^2[1-(1-a^L)^{L-2}(1-4a^L-a^{2L})] \\ -4(L-1)a^L(1-a^L)^{L-2}[a(1-a^{L-1})/(1-a)]. \tag{A2.10}$$

This yields, for large L,

$$X \sim 2\lambda_1, \tag{A2.11}$$

and the normalised eigenvector is $(2/\sqrt{5})[^{-1}_{\frac{1}{2}}]$. This is not the direction $[^{-1}_{1}]$ of the exact critical line (Sykes and Essam 1963). Clearly, there is an unusual singularity for the cell PSRG at (1, 0) as $L \to \infty$ where the three fixed points D_1, D_2, and D_3 merge.

Appendix 3. Large-L behaviour of decimation PSRG

For the decimation scheme discussed in § 2.2, the recursion relation for a can be expressed for a general rescaling length L as

$$a' = a^L(1-a)^{L^2}R_L(b) + \cdots + a^{L(L+1)-1}(1-a)R_{L(L+1)-1}(b) + a^{L(L+1)} \tag{A3.1}$$

where $R_i(b)$ are polynomials in b. Thus we find

$$(\partial a'/\partial b)|_{a=1} = (\partial a'/\partial a)|_{a=0} = (\partial a'/\partial b)_{a=0} = 0, \tag{A3.2}$$

as well as

$$a'|_{a=1} = 1, \qquad a'|_{a=0} = 0. \tag{A3.3}$$

Thus, the flows originating on the edges of the diagram (cf figure 4) are constrained to lie on the edge. It is also easy to show

$$(\partial a'/\partial a)|_{a=b=1} = [-a^{L(L+1)-1}R_{L(L+1)-1}(b) + L(L+1)a^{L(L+1)-1}]_{a=b=1} = 0. \tag{A3.4}$$

Thus

$$T_L(B) = T_L(C) = \mathbf{0} \tag{A3.5}$$

for all L, and also

$$T_L(D_1) = \begin{bmatrix} L(L+1) - R_{L(L+1)-1}(b=0) & 0 \\ 0 & 0 \end{bmatrix} = \begin{bmatrix} L & 0 \\ 0 & 0 \end{bmatrix}. \tag{A3.6}$$

This shows that both B and C are infinite sinks in all directions, while D_1 is an infinite sink only in the b direction. In the a direction, we find that D_1 has a scaling power y_1 of unity for all L. In other words, D_1 describes the one-dimensional behaviour correctly (as is easy to see since $a'(b=0) = a^L$).

We now consider the non-trivial fixed point D_2 on the edge $a = 1$. When $a = 1$, the recursion relation for b becomes

$$b' = [1-(1-b)^{L+1}]^L. \tag{A3.7}$$

By letting $r = b^*$, we see that $r \to 0$ as $L \to \infty$, and that we have the same problem as in appendix 2. Hence

$$b^* \sim (\ln L - \ln\ln L)/L. \tag{A3.8}$$

Next, we focus our attention on the linearised recursion relations at D_2. We have

$$T_L(D_2) = \begin{bmatrix} \lambda_1 & 0 \\ X & \lambda_2 \end{bmatrix}, \tag{A3.9}$$

where λ_1 is the eigenvalue associated with the (right) eigenvector $\begin{bmatrix} -1 \\ X/(\lambda_2-\lambda_1) \end{bmatrix}$, and λ_2 with $\begin{bmatrix} 0 \\ 1 \end{bmatrix}$. For all even L, it is straightforward but tedious to show that

$$\lambda_1 = L - \sum^{L} x_i(2-x_i) \qquad (x_i \equiv [1-(1-b^*)^i][1-(1-b^*)^{L+1-i}]), \tag{A3.10}$$

$$\lambda_2 = L(L+1)(1-b^*)^L[1-(1-b^*)^{L+1}]^{L-1} \tag{A3.11}$$

and

$$\begin{aligned} X = {} & L(L+1)h^L - L(L-1)h^L + 2L(L-1)(1-h)h^{L-2}(2-h) \\ & - 4(L-1)(1-b^*)^{L+2}h^{L-2}[1-(1-b^*)^L]/b^* \\ & + 4(1-b^*)^{L/2+1}h^{L-1}[1-(1-b^*)^{L/2}]b^* - 2Lh^{L-1} \end{aligned} \tag{A3.12}$$

where

$$h^L \equiv [1-(1-b^*)^{L+1}]^L.$$

For example, we find for the case $L=2$ (figure 4), $b^*=0.152$, $\lambda_1=1.83$ and $\lambda_2=1.68$, with the corresponding scaling powers $y_1=0.87$ and $y_2=0.75$. Both of these numbers are close to $1/\nu_{d=1}=1$, and thus reasonable. However, we must consider these quantities as $L\to\infty$ to find possible systematic improvement. An analysis similar to that in appendix 2 yields

$$y_1 \sim 1 - \ln\ln L/\ln L \to 1, \tag{A3.13}$$

$$y_2 \sim 2\ln\ln L/\ln L \to 0. \tag{A3.14}$$

From (A3.12), clearly X does not grow as fast as $L\ln L$. In fact, X grows no faster than $2\ln L$. In addition λ_1 dominates in $(\lambda_2-\lambda_1)$. Thus we have

$$|X/(\lambda_2-\lambda_1)| \sim 2(\ln L)^2/L \tag{A3.15}$$

and

$$\begin{bmatrix} -1 \\ X/(\lambda_2-\lambda_1) \end{bmatrix} \to \begin{bmatrix} -1 \\ 0 \end{bmatrix}.$$

Therefore, while y_1 approaches the one-dimensional value of unity, its (right) eigenvector approaches $\begin{bmatrix} -1 \\ 0 \end{bmatrix}$; the scaling power y_2, however, goes to zero in this decimation scheme, making the eigenvector $\begin{bmatrix} 0 \\ 1 \end{bmatrix}$ marginal in the asymptotic limit.

References

Abe R 1970 *Prog. Theor. Phys.* **44** 339–47

Aharony A 1976 in *Phase Transitions and Critical Phenomena* ed. C Domb and M S Green (New York: Academic) vol 6 pp 357–424

Chaves C M, Oliveira P M and de Queiroz S L A 1979 *Prog. Theor. Phys.* **62** 1550–5

Coniglio A, Stanley H E and Klein W 1979 *Phys. Rev. Lett.* **42** 518–22

de Gennes P G 1979 *Scaling Concepts in Polymer Physics* (Ithaca: Cornell University)

Ikeda H 1979 *Prog. Theor. Phys.* **61** 842–9

Kasteleyn P W and Fortuin C M 1969 *J. Phys. Soc. Japan Suppl.* **26** 11–4

McCoy B M and Wu T T 1973 *The two-dimensional Ising model* (Cambridge: Harvard University)

de Magalhães A C N, Tsallis C and Schwachheim G 1980 *Preprint*

Niemeijer T and van Leeuwen J M J 1976 in *Phase Transitions and Critical Phenomena* ed. C Domb and M S Green vol 6

Onsager L 1944 *Phys. Rev.* **65** 117
Redner S and Coniglio A 1980 *Phys. Lett.* **79**A 111–2
Redner S and Stanley H E 1979 *J. Phys. A: Math. Gen.* **12** 1267–83
Reynolds P J, Klein W and Stanley H E 1977 *J. Phys. C: Solid State Phys.* **10** L167–72
Reynolds P J, Stanley H E and Klein W 1980 *Phys. Rev.* B**21** 1223–45
Reidel E and Wegner F 1969 *Z. Phys.* **225** 195–215
Suzuki M 1971 *Prog. Theor. Phys.* **46** 1054–70
Sykes M F and Essam J W 1963 *Phys. Rev. Lett.* **10** 3–4
Temperley H N V and Lieb E H 1971 *Proc. Phys. Soc.* A **322** 251–80
Turban L 1979 *J. Phys. A: Math. Gen.* **12** 1–12